Hydrolysis Studies of Chalcogenopyrylium Trimethine Dyes. 2. Chalcogen Atom Effects on the Rates of Hydrolysis of Chalcogenopyrylium Dyes

David N. Young, Petr Serguievski,* and Michael R. Detty*

Department of Medicinal Chemistry, School of Pharmacy, SUNY at Buffalo, Buffalo, New York 14260

Received April 21, 1998

Dyes with near-infrared-absorbing chromophores compatible with near-infrared-emitting diode lasers are becoming increasingly important in applications of technology such as charge-generation in electrophotography, heat generation in optical recording and thermal imaging, sensitization of silver halide emulsions for near-infrared photography, and filter systems for near-infrared-emitting diode lasers.[1−3] Medical technology has found near-infrared-absorbing dyes useful as sensitizers for photodynamic therapy (PDT).[4,5] Certainly two of the more useful dye chromophores have been the chalcogenopyrylium and benzochalcogenazolium dyes (**1** and **2**, respectively) as well as benzo- and dibenzo analogues of the former (**3** and **4**, respectively).[1−3]

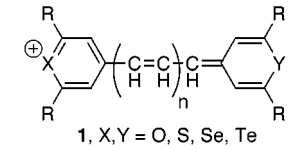

1, X,Y = O, S, Se, Te

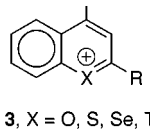

3, X = O, S, Se, Te

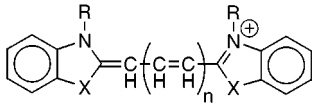

2, X = O, S, Se, Te

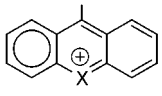

4, X = O, S, Se, Te

The hydrolytic stability of the dyes is a key factor in their lifetime and utility in the applications described above, as well as in related applications. In electronic and imaging applications of such dyes, the hydrolytic stability impacts shelf life, the working lifetime of the device, formulation, and packaging. In PDT, the kinetics of hydrolysis of the dyes affect the circulating lifetime of the drug in vivo as well as the shelf life of formulations to deliver them, while the products of hydrolysis define potential in vivo metabolites.

Scheme 1

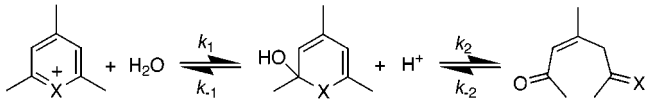

6a, X = O
6b, X = S

7a, X = O
7b, X = S

8a, X = O
8b, X = S

In dyes **1**−**4**, the chalcogen atom(s) are an integral part of the π-framework of the dye and will influence not only photophysical but also chemical properties of the chromophore. One electronic effect is that the maxima of absorption move to longer wavelengths as lighter chalcogen atoms are replaced by heavier chalcogen atoms.[1−3] We have been investigating the effects of chalcogen atoms on the regiochemistry and kinetics of hydrolysis for the dye series **5**, with absorption maxima in water between 595 nm (**5a**) and 810 nm (**5f**). The products of hydrolysis of dyes **5** under conditions at pH 8 were recently described.[6] The regiochemistry of hydrolysis was dependent on the identity of the heteroatoms, with dye **5a** giving mostly (>93%) products from H_2O/HO^- addition to the 2-position of the pyrylium ring and dye **5f** giving more than 60% of products from the addition to the central carbon of the trimethine bridge.[6] In this paper, we examine the hydrolysis of the dye series **5** with respect to the effects of the different chalcogen atoms on the rates of hydrolysis.

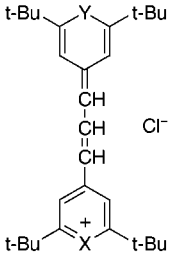

5a, X = Y = O
5b, X = Se, Y = O
5c, X = Te, Y = O
5d, X = Y = S
5e, X = Y = Se
5f, X = Y = Te

Results and Discussion

The hydrolyses of a variety of simple pyrylium[7] and thiopyrylium[8] salts **6** have been described in detail and the processes involved are summarized in Scheme 1. Products were formed by addition of H_2O/HO^- to the 2-position of the pyrylium or thiopyrylium nucleus to give alcohols **7** (with proton release from water addition).[7,8] Rearrangement of **7** gives the 2-pentene-1,5-diones **8a**[7]

(1) Matsuoka, M., Ed. *Infrared Absorbing Dyes*; Plenum Press: New York, 1990.

(2) Detty, M. R.; O'Regan, M. B. *Tellurium Containing Heterocycles*; The Chemistry of Heterocyclic Compounds; Taylor, E. C., Ed.; Wiley-Interscience: New York, 1994; Vol. 53.

(3) Doddi, G.; Ercolani, G. *Adv. Heterocycl. Chem.* **1994**, *60*, 65−195.

(4) PDT is a recent development in the treatment of cancer in which a cytotoxic agent (singlet oxygen, superoxide, radicals) is produced in vivo by the irradiation of a tumor-localized photochemical sensitizer: (a) Rosenthal, D. I.; Glatstein, E. *Ann. Medicine* **1994**, *26*, 405. (b) Henderson, B. W.; Dougherty, T. J., Eds. *Photodynamic Therapy: Basic Principles and Clinical Aspects*; Marcel Dekker: New York, 1992; pp 1−459. (c) Penning, L. C.; Dubbelman, T. M. *Anti-Cancer Drugs* **1994**, *5*, 139. (d) Cannon, J. B. *J. Pharmaceut. Sci.* **1993**, *82*, 435−446. (e) Pass, H. I. *J. Nat. Cancer Inst.* **1993**, *85*, 443.

(5) (a) Detty, M. R.; Merkel, P. B.; Hilf, R.; Gibson, S. L.; Powers, S. K. *J. Med. Chem.* **1990**, *33*, 1108−1116. (b) Modica-Napolitano, J. S.; Joyal, J. L.; Ara, G.; Oseroff, A. R.; Aprille, J. R. *Cancer Res.* **1990**, *50*, 7876−7881. (c) Powers, S. K.; Walstad, D. L.; Brown, J. T.; Detty, M. R.; Watkins, P. J. *J. Neurooncol.* **1989**, *7*, 179−183. (d) Kessel, D. *Photochem. Photobiol.* **1991**, *53*, 73−78.

(6) Young, D. N.; Detty, M. R. *J. Org. Chem.* **1997**, *62*, 4692−4700.

(7) (a) Balaban, A. T.; Dinculescu, A.; Dorofeenko, G. N.; Fischer, G. W.; Koblik, A. V.; Mezheritskii, V. V.; Schroth, W. *Pyrylium Salts: Syntheses, Reactions, and Physical Properties*; Advances in Heterocyclic Chemistry, Supplement 2; Katritzky, A. R., Ed.; Academic Press: New York, 1982; pp 66−73. (b) Williams, A. *J. Am. Chem. Soc.* **1971**, *93*, 2733−2737. (c) Salvadori, G.; Williams, A. *J. Am. Chem. Soc.* **1971**, *93*, 2727−2733.

(8) (a) Degani, I.; Fochi, R.; Vincenzi, C. *Gazz. Chim. Ital.* **1967**, *97*, 397. (b) Pedersen, C. L. *Acta Chem. Scand, Ser. B* **1975**, *B29*, 453. (c) Khbeis, S. G.; Maas, G.; Regitz, M. *Tetrahedron* **1985**, *41*, 811.

S0022-3263(98)00742-7 CCC: $15.00
Published on Web 07/23/1998

Scheme 2

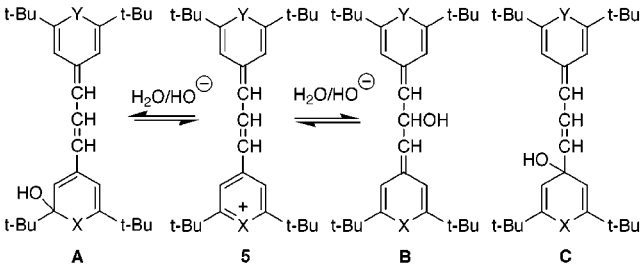

or keto thioenols **8b**.[8] (Under more basic conditions, compounds **8b** may be hydrolyzed to diones **8a**.)[8] The second step of the reaction is written as an equilibrium since treatment of products **8** with acid regenerates the corresponding pyrylium or thiopyrylium nucleus.[7,8] The observed rate constant for hydrolysis, k_{obs}, is a composite of the rate constants for all of these steps. For simple pyrylium and thiopyrylium nuclei, k_{obs} increases as pH increases with a plateau region around pH 6, the onset of which corresponds to the pK_a of the pyrylium and thiopyrylium salts.

Hydrolysis studies of trimethine dyes **5** (as well as other methine and polymethine dyes) are complicated by several potential sites of addition of H_2O/HO^-, as shown in Scheme 2. Product studies have shown that both A and B are involved in product formation with dyes **5**.[6] Although hydrolysis products derived from alcohol C have not been observed, one would expect H_2O/HO^- addition to be competitive at this site as well. The various alcohols are in equilibrium with each other and with the starting dye **5**. With unsymmetrical dyes **5** (X ≠ Y), two additional sites of addition are possible in the second ring.

Kinetics of Hydrolysis. The rates of hydrolysis for the dyes **5** of this study were measured at 310.0 ± 0.1 K in phosphate-buffered, aqueous solutions (pH range 1.75−12.5) at nearly constant potassium ion concentration, [K^+], and ionic strength, μ. Values of k_{obs} for dyes **5a**−**c** containing a pyrylium ring are compiled in Table 1[9] and for symmetrical thiopyrylium (**5d**), selenopyrylium (**5e**), and telluropyrylium dyes (**5f**) in Table 2. Decays of the characteristic absorption bands of the dyes were fit to single-exponential functions. The values given in Tables 1 and 2 represent the average of three or more runs with error limits of ±2σ.

Hydrolysis of Dyes 5a−c Containing a Pyrylium Ring. Product studies have shown that dyes **5a**−**c**, containing a pyrylium nucleus, all give enediones as the predominant products (≥90%) as shown in Scheme 3.[6] Addition of water/hydroxide to the 2-position of the pyrylium ring gives hemiacetals **9**. Hemiacetals **9** can regenerate the corresponding dye **5** by reaction with a proton to give dehydration or can rearrange to give enediones **10**. Product studies at pH 8 indicate that enediones **10** are the only end products of hydrolysis under alkaline conditions (although enediones **10** can undergo self-condensation reactions at high pH),[6] which is analogous to product studies with other pyrylium systems.[7,8]

Values of log k_{obs} (Table 1) are plotted as a function of pH for dyes **5a**−**c** in Figure 1. The rates of hydrolysis of dyes **5** increased with pH, and plots of log k_{obs} vs pH display distinct plateau regions at approximately pH 8−11 for **5a**, pH 6−9 for **5b**, and pH 6−10 for **5c**. Rates of hydrolysis away from the plateau regions are nearly identical in all three systems, suggesting that the second chalcogen atom has little impact on the rates of hydrolysis away from the plateau regions.

Table 1. Values of k_{obs} (±2σ) for Hydrolysis of Dyes 5a−c Containing a Pyrylium Ring as a Function of pH at 310.0 ± 0.1 K in Buffered Aqueous Solutions

	k_{obs}, s^{-1}		
pH	dye **5a**[a]	dye **5b**[b]	dye **5c**[c]
1.75	$(6.0 \pm 0.5) \times 10^{-7}$		
3.2		$(6.2 \pm 0.3) \times 10^{-7}$	
4.2	$(1.4 \pm 0.6) \times 10^{-7}$		$(1.05 \pm 0.06) \times 10^{-5}$
4.5		$(2.4 \pm 0.7) \times 10^{-6}$	
5.2		$(4.9 \pm 0.3) \times 10^{-6}$	$(3.3 \pm 0.2) \times 10^{-5}$
5.7			$(1.21 \pm 0.05) \times 10^{-4}$
6.0			$(2.7 \pm 0.1) \times 10^{-4}$
6.1	$(2.9 \pm 0.6) \times 10^{-5}$	$(6.2 \pm 0.5) \times 10^{-5}$	
7.0			$(7.4 \pm 0.4) \times 10^{-4}$
7.2	$(1.6 \pm 0.3) \times 10^{-4}$	$(1.0 \pm 0.1) \times 10^{-4}$	
7.75	$(6.3 \pm 0.6) \times 10^{-4}$		
8.2	$(1.1 \pm 0.5) \times 10^{-3}$	$(4.2 \pm 0.3) \times 10^{-4}$	$(1.3 \pm 0.1) \times 10^{-3}$
9.0	$(1.3 \pm 0.5) \times 10^{-3}$		$(1.8 \pm 0.1) \times 10^{-3}$
9.3		$(1.8 \pm 0.6) \times 10^{-3}$	
9.7	$(2.5 \pm 0.1) \times 10^{-3}$		
11.0	$(4 \pm 1) \times 10^{-3}$	$(1.10 \pm 0.04) \times 10^{-2}$	$(1.7 \pm 0.3) \times 10^{-2}$
12.1	$(8.06 \pm 0.09) \times 10^{-2}$	$(1.2 \pm 0.1) \times 10^{-1}$	$(1.2 \pm 0.1) \times 10^{-1}$

[a] Measured at 595 nm. [b] Measured at 645 nm. [c] Measured at 710 nm.

Table 2. Values of k_{obs} (±2σ) for Hydrolysis of 5d−f as a Function of pH at 310.0 ± 0.1 K in Buffered Aqueous Solutions

	k_{obs}, s^{-1}		
pH	dye **5d**[a]	dye **5e**[b]	dye **5f**[c]
3.2	$(2.8 \pm 0.3) \times 10^{-6}$		
3.5		$(2.4 \pm 0.2) \times 10^{-6}$	$(1.46 \pm 0.09) \times 10^{-5}$
4.5	$(2 \pm 1) \times 10^{-7}$	$(2.2 \pm 0.7) \times 10^{-6}$	$(3.0 \pm 0.6) \times 10^{-5}$
5.5	$(3 \pm 2) \times 10^{-7}$		
6.1		$(1.46 \pm 0.08) \times 10^{-5}$	$(5 \pm 1) \times 10^{-5}$
6.3	$(7 \pm 6) \times 10^{-7}$		
6.9	$(3 \pm 2) \times 10^{-6}$		
7.2	$(7 \pm 4) \times 10^{-6}$	$(4.3 \pm 0.5) \times 10^{-5}$	$(1.8 \pm 0.2) \times 10^{-4}$
7.7	$(2 \pm 1) \times 10^{-5}$		
8.2		$(1.2 \pm 0.3) \times 10^{-4}$	$(3.7 \pm 0.6) \times 10^{-3}$
8.35	$(1.7 \pm 0.3) \times 10^{-5}$		
9.2	$(2 \pm 1) \times 10^{-5}$		
9.3		$(2.3 \pm 0.2) \times 10^{-4}$	$(5.0 \pm 0.2) \times 10^{-2}$
9.8	$(8.6 \pm 0.9) \times 10^{-5}$		$(1.36 \pm 0.01) \times 10^{-1}$
11.0	$(1.3 \pm 0.5) \times 10^{-4}$	$(1.35 \pm 0.01) \times 10^{-2}$	$(7.50 \pm 0.05) \times 10^{-1}$
11.2	$(2.2 \pm 0.3) \times 10^{-4}$		
12.1	$(1.7 \pm 0.5) \times 10^{-3}$	$(8.22 \pm 0.02) \times 10^{-2}$	$(2.96 \pm 0.04) \times 10^{1}$
12.5	$(3.3 \pm 0.5) \times 10^{-3}$	$(3.98 \pm 0.07) \times 10^{-1}$	

[a] Measured at 650 nm. [b] Measured at 730 nm. [c] Measured at 810 nm.

Scheme 3

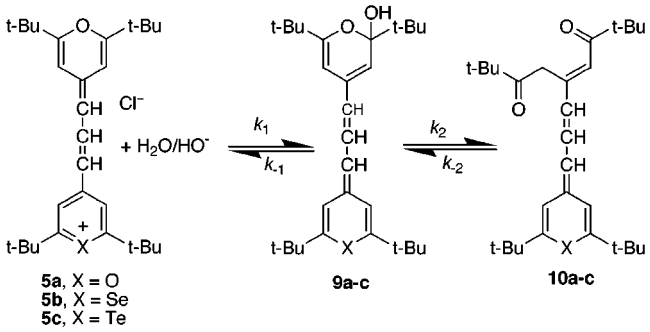

(9) The mixed pyrylium/thiopyrylium dye **5g** (X = S, Y = O) was isolated in 85% purity with **5a** and **5d** as contaminants in nearly equal amounts (≈7% each). This dye was not included in the kinetic studies. Such heteroatom scrambling has been described: Detty, M. R.; Young, D. N.; Williams, A. J. *J. Org. Chem.* **1995**, *60*, 6631−6635.

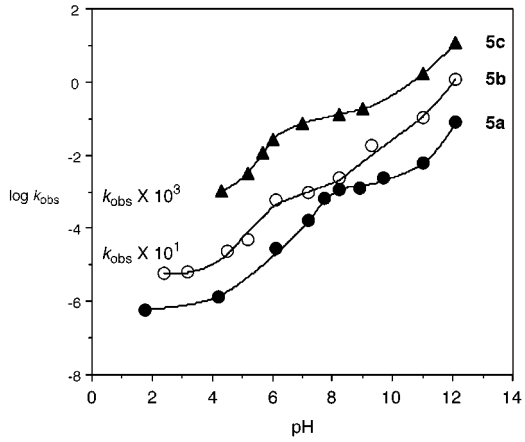

Figure 1. A plot of log k_{obs} as a function of pH for pyrylium dyes **5a** (filled circles), **5b** (open circles), and **5c** (filled triangles). For clarity, k_{obs} has been multiplied by a factor of 10^1 for **5b** and 10^3 for **5c**. The lines shown are interpolated between points and have no physical significance. Error bars for individual rates have been omitted for clarity, but errors ($\pm 2\sigma$) are listed in Table 1.

The reversibility of Scheme 3 (and reality of k_{-2}) was demonstrated by acidification of the alkaline hydrolysis solution after approximately two half-lives of hydrolysis. A thin glass rod was dipped into 60% HPF_6 and the acid-coated rod was used to stir a cuvette containing dye **5a** and a dilute pH 8.0 buffer. The pH of the solution in the cuvette was lowered to pH 3−4 and the increase in absorbance at 595 nm was noted. We assumed that the pH change drove the equilibrium of alcohol **9a**, dione **10a**, and **5a** to the left. (Introduction of a second acid treatment did not change the absorbance at 595 nm). The average absorbance following acidification of the hydrolysis mixture for five runs was 0.85 ± 0.12, while the average initial absorbance at pH 8.0 for these runs was 0.88 ± 0.06. Absorbance at the time of acidification was 0.25 ± 0.05. Similar results were obtained with dye **5b**, as observed at 645 nm. The average absorbance following acidification of the hydrolysis mixtures of **5b** for five runs was 0.8 ± 0.1, while the average initial absorbance at pH 8.0 for these runs was 0.93 ± 0.05. Absorbance at the time of acidification of the hydrolysis mixture of **5b** was 0.25 ± 0.05.

The plateau regions are related to the pK_as of the chalcogenopyrylium dyes **5** and suggest either that an intermediate deprotonates to give a reactive species or that an intermediate is formed with the simultaneous release of a proton. Similar log k_{obs} vs pH profiles have been observed with simple pyrylium and thiopyrylium systems.[7,8] In these systems, it was argued that increasing pK_as indicate increased stability (more aromaticity) in the substituted pyrylium and thiopyrylium rings. 2,4,6-Triphenylpyrylium tetrafluoroborate and 2-methyl-4,6-diphenylpyrylium chloride have acidities (p$K_a \approx 6$) similar to that of acetic acid, while 2,4,6-trimethylpyrylium is somewhat more acidic.[7b] These results were interpreted to suggest increased stabilization of the pyrylium nucleus by phenyl substituents. On the basis of plateau regions of the log k_{obs} vs pH profiles, dyes **5b** (p$K_a \approx 6.5$) and **5c** (p$K_a \approx 6$) are comparable in acidity to 2,4,6-triphenylpyrylium tetrafluoroborate and 2-methyl-4,6-diphenylpyrylium chloride, while **5a** (p$K_a \approx 8$) is significantly less acidic. These data suggest a greater stability for the pyrylium dye chromophore in **5a** relative to simple pyrylium and thiopyrylium salts (the equilibria of Scheme 3 lie further to the left relative to those of Scheme 1).

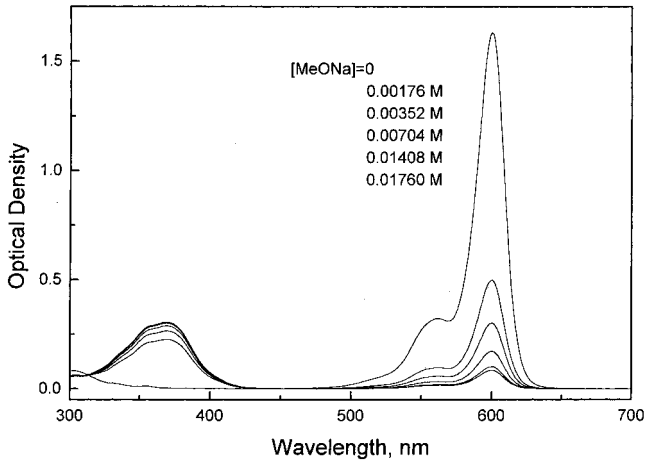

Figure 2. Equilibrium addition of MeO^- (0, 1.76×10^{-3}, 3.52×10^{-3}, 7.04×10^{-3}, 1.41×10^{-2}, 1.76×10^{-2} M) to **5a** (6.7×10^{-6} M) in MeOH at 310.0 ± 0.1 K. The 595-nm band is decreasing and the 370-nm band is increasing with increasing CH_3O^- concentration.

Since the enedione products **10** are formed from hydroxide/water addition to the pyrylium ring followed by rearrangement, the contributions to k_{obs} from the second chalcogen atom will be primarily electronic in nature. The onset of the plateau region for pyrylium dye **5a** is observed at approximately 2 pH units higher than those of selenopyrylium dye **5b** and telluropyrylium dye **5c**, which suggests that **5a** is thermodynamically more stable than **5b** and **5c**. In terms of chalcogen atom size, overlap of the Se 4p orbital in **5b** and the Te 5p orbital in **5c** with the carbon π-framework should be much less effective than overlap of the O 2p orbitals of **5a** with the π-framework. The poorer overlap reduces the aromaticity of the contributions from selenopyrylium and telluropyrylium rings in dyes **5b** and **5c** and, consequently, renders these dyes more reactive toward addition of H_2O/HO^- at a lower pH than observed for **5a**.

Stopped-Flow Studies with Dyes 5a−c. According to Scheme 3, the shape of the kinetic profile of the hydrolysis process of dyes **5a−c** depends on the relative magnitudes of the rate constants k_1, k_{-1}, k_2, and k_{-2}. Namely, if $k_1[HO^-] > (k_{-1} + k_2)$ at higher pH values, the reaction is expected to show a fast initial component followed by a slower step. In this case, an intermediate formed upon the addition of H_2O/HO^-, usually referred to as a pseudobase,[7,10] accumulates in the system. Attainment of the reaction conditions favorable for such accumulation would permit identification of the absorption spectrum of the pseudobase as well as allow for an estimation of rate constants for addition of HO^- to a pyrylium ring. A similar situation has been observed in the hydrolysis of 1,3-diphenyl-2-imidazolium chloride by Robinson.[11] In that system, a two-component decay profile was observed at high pH values. By following the reasoning presented in that work, it was expected that similar behavior might be observed in the hydrolysis of **5a** at high pH.

(10) Bunting, J. W. Heterocyclic Pseudobases. In *Advances in Heterocyclic Chemistry*; Katritzky, A. R., Boulton, A. J., Eds.; Academic Press: New York, 1982; Vol. 25, pp 1−79.

(11) Robinson, D. R. *J. Am. Chem. Soc.* **1970**, *92*, 3138−3146.

To help in the identification of the pseudobase intermediate, its absorption spectrum in MeOH was estimated by allowing dye **5a** to react with MeO^-. The species formed by addition of MeO^- to the 2-position in the pyrylium ring is incapable of rearrangement to yield ring-opened products, and its spectral characteristics should be similar to its analogue formed by the addition of HO^-.[10] A 6.7×10^{-6} M solution of **5a** in MeOH was allowed to equilibrate in the presence of various concentrations of NaOMe (Figure 2).[12] As the concentration of NaOMe increased, the absorption of the dye at 600 nm decreased, accompanied by an increase in absorption in the 350−400-nm region with a maximum at 370 nm. Clean isosbestic behavior was observed. The new absorption bands were attributed to the formation of pseudobase **11** from the addition of MeO^- to **5a**. Our

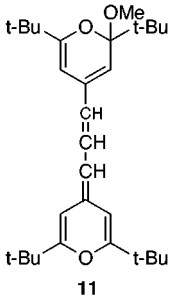

11

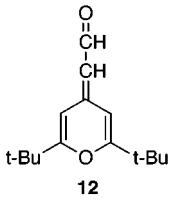

12

structural assignment was based on the absorption maximum of 335 nm observed for **12**[13] in MeOH. One would expect addition of MeO^- either to the central carbon of the trimethine bridge or to the 4-position of the pyrylium ring of **5a** to give a chromophore with a maximum shorter than 370 nm.

Stopped-flow experiments were carried out in a mixed CH_3CN-H_2O solvent (44 wt % of CH_3CN) to ensure that all components of the reaction were completely solubilized. Various amounts of KOH were dissolved in the solvent and allowed to mix in the mixing chamber of the stopped-flow instrument with a 7.9×10^{-6} M solution of the dye in 0.005 M HCl. Kinetics of the reaction were followed by recording absorption−change profiles every 5 nm between 320 and 630 nm. The final concentration of KOH varied between 0.0165 and 0.0755 M. The pH of these solutions, adjusted for the mixed-solvent system,[14] varied from 11.60 to 12.21. Upon mixing, an immediate disappearance of the main absorption bands of the dye was observed accompanied by a concomitant growth of absorption around 450 nm (Figure 3). A clean isosbestic point was observed at 515 nm. *Single-exponential kinetics were observed at 450 and 595 nm from the first milliseconds of reaction through at least five half-lives ($t_{1/2} \approx 10-80$ s) for all values of [HO⁻].* No accumulation of an intermediate could be detected as absorption changes at 370 nm followed those at 450 nm. It is extremely unlikely that the species absorbing in the 450 nm region is the pseudobase intermediate. Its spectrum in CH_3CN-H_2O mixture is not expected to differ significantly from that in methanol. Furthermore,

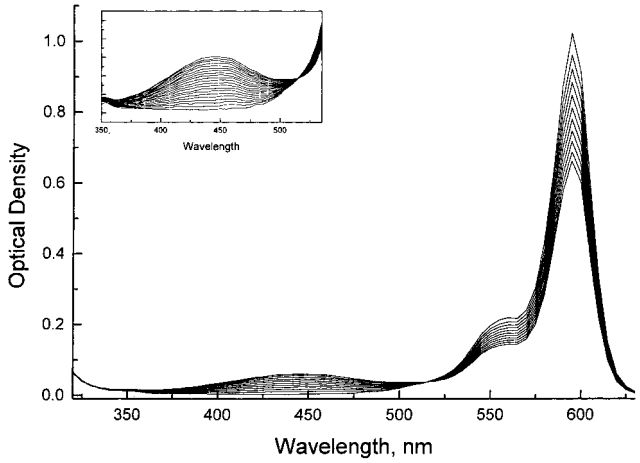

Figure 3. Hydrolysis of **5a** at pH 11.60 in 44 wt % CH_3CN-H_2O at 310.0 ± 0.1 K. Absorption spectra are 3 s apart with the 595-nm band decreasing with time and the 450-nm band increasing with time. An isosbestic point is observed at 515 nm. The final trace is after 3600 s. Absorption spectra at indicated time points were calculated through software provided by Applied Photophysics. This consisted of slicing at the appropriate time points across a series of kinetic traces (at 5-nm intervals between 320 and 630 nm) and then splining the points of a specific time group.

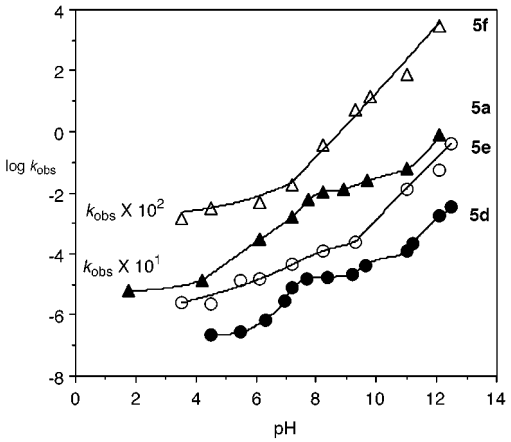

Figure 4. A plot of log k_{obs} as a function of pH for symmetrical chalcogenopyrylium dyes **5a** (filled triangles), **5d** (filled circles), **5e** (open circles), and **5f** (open triangles). For clarity, k_{obs} has been multiplied by a factor of 10^1 for **5a** and 10^2 for **5f**. The lines shown are interpolated between points and have no physical significance. Error bars for individual rates have been omitted for clarity, but errors ($\pm 2\sigma$) are listed in Tables 1 and 2.

the yellow color of the solutions produced by the species absorbing in the 450 nm region persisted for days, thus supporting the argument that this species is the final product of the hydrolysis, i.e., the enedione **10a**.

These observations suggest that the processes defined by $(k_{-1} + k_2)$ are faster than the addition of OH^-. The rate constant k_1 cannot, therefore, be directly determined from the kinetic data. The rate constant for the addition of hydroxide ion to the carbon atom of the imidazolium ring has been measured at 1.6×10^4 M^{-1} s^{-1} in water by Robinson,[11] while Williams has determined the corresponding rate constant for HO^- addition to the 2-position of trimethylpyrylium to be 1.3×10^4 M^{-1} s^{-1}.[7b] On the basis of the known values of $\{pK_{R+}\}$ for pyrylium derivatives,[10] k_{-1} is estimated to be small. Therefore, k_2 is expected to be faster than k_1 for the dye **5a**. One would

(12) The addition of NaOMe to 2,6-di-*tert*-butyl-4-methylthiopyrylium tetrafluoroborate in MeOH has been described under equilibrium conditions: Doddi, G.; Ercolani, G. *J. Chem. Soc., Perkin Trans. 2* **1989**, 1393−1396.

(13) Wadsworth, D. H.; Detty, M. R.; Murray, B. J.; Weidner, C. H.; Haley, N. F. *J. Org. Chem.* **1984**, *49*, 2676−2681.

(14) Marcus, Y. *Ion Solvation*; Wiley and Sons: New York, 1985.

expect the k_{-1} term to decrease as the size of the chalcogen atom in the ring increases. The aromaticity of the chalcogenopyrylium ring decreases with heteroatom size due to poorer overlap of orbitals between π-framework and heteroatom.[2] Consequently, the driving force to dehydrate and rearomatize (k_{-1}) should decrease with chalcogen atom size.

Hydrolysis of Symmetrical Chalcogenopyrylium Dyes 5a and 5d−f. Values of log k_{obs} (Tables 1 and 2) are plotted as a function of pH for symmetrical (X = Y) dyes **5a** and **5d−f** in Figure 4. Interestingly, the presence or absence of a plateau region in the log k_{obs}−pH profiles correlated with the hydrolysis product distribution. Pyrylium dye **5a** and thiopyrylium dye **5d** give hydrolysis products primarily derived from alcohol **A** of Scheme 2[6] and give k_{obs}−pH profiles with distinct plateau regions (Figure 4, pH 7−10 for **5d**). Selenopyrylium dye **5e** gives a mixture of enedione **10b** (from addition of hydroxide/water to the 2-position of the selenopyrylium ring followed by hydrolysis of the resulting selenoketone **13a**) and **14a** and **15a** (from addition of hydroxide/water

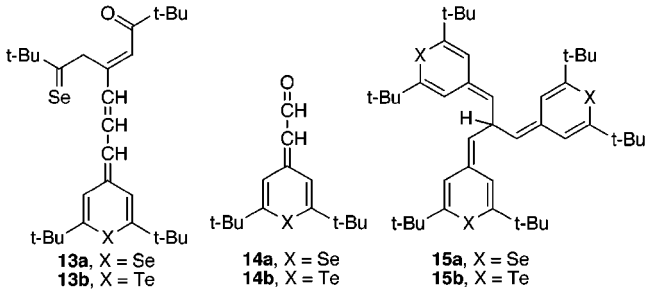

to the central carbon of the trimethine bridge).[6] None of these products are in equilibrium with **5e**, as recyclization of **10b** generates **5b** and not **5e**. Similarly, telluropyrylium dye **5f** gives **13b** and **14b** irreversibly as the major hydrolysis products (from addition of hydroxide/water to the central carbon of the trimethine bridge).[6]

Of the four dyes, telluropyrylium dye **5f** is the most reactive toward hydrolysis while thiopyrylium dye **5d** is the least reactive toward hydrolysis over the pH range of 3−12. The thiopyrylium dye is slower to hydrolyze by a factor of 10^1−10^2 relative to the other dyes **5** over the pH range of 3−12.

Summary and Conclusions

Chalcogenopyrylium dyes behave as weak acids in aqueous systems by generating a proton upon addition of water. For dyes **5a−d**, which reversibly form an enedione (or eneone−thione for **5d**) as the conjugate base, plots of log k_{obs} vs pH show a plateau, as is observed in Figures 1 and 4 with the onset of the plateau corresponding to the pK_a of the dye. *Beyond this buffering region and for dyes **5e** and **5f** with irreversible hydrolysis, one would expect the log k_{obs} vs pH profiles to be a series of parallel lines with a slope of 1 at higher values of pH as k_{obs} is dominated by the k_{OH}[OH] term*. Of the dyes examined in this study, thiopyrylium dye **5d** gives a linear response for the k_{obs} vs pH profile in the pH 11.0−12.5 range with a slope of 0.95 ± 0.04, selenopyrylium dye **5e** gives a linear response for the k_{obs} vs pH profile in the pH 9.3−12.5 range with a slope of 0.97 ± 0.07, and telluropyrylium dye **5f** gives a linear response for the k_{obs} vs pH profile in the pH 7.2−12.1 range with a slope of 1.00 ± 0.06 (Figure 5). Hydrolyses of the other dyes in this study were not dominated by the k_{OH}[OH] term at the higher pHs. One can *approximate* the second-order rate constants for k_{OH} for dyes **5d−f** from the intercepts of the linear regions of Figure 5 (−14.3 ± 0.5, −12.6 ± 0.8, and −10.8 ± 0.6, respectively, for **5d−f**; at pH 0, [OH] = 10^{-14} M), which gives values of k_{OH} between 0.2 and 1.6 M^{-1} s^{-1} for **5d**, between 4 and 130 M^{-1} s^{-1} for **5e**, and between 410 and 6200 M^{-1} s^{-1} for **5f**.

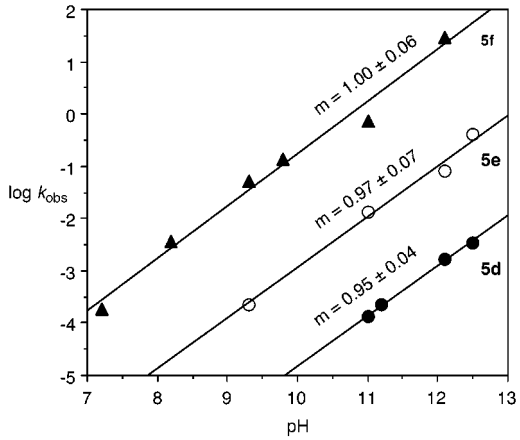

Figure 5. Linear regions for the hydrolyses of **5d−f** where the k_{OH}[OH] term is dominant. Slopes (±σ) as determined by least-squares analysis are indicated with intercepts of −14.3 ± 0.5 for **5d**, −12.6 ± 0.8 for **5e**, and −10.8 ± 0.6 for **5f**. Correlation coefficients are R^2 = 0.996 for **5d**, 0.99 for **5e**, and 0.99 for **5f**. Error bars for individual rates have been omitted for clarity, but errors (±2σ) are listed in Table 2.

The qualitative ordering of these rates can be best rationalized in terms of higher stability (aromaticity) of the thiopyrylium ring relative to the selenopyrylium ring, which in turn is more stable than the telluropyrylium ring.[2] In chalcogenopyrylium compounds, increasing the size of the chalcogen atom decreases the effectiveness of orbital overlap in the π-framework. One would expect telluropyrylium dyes to be most reactive and pyrylium dyes the least based on this trend. In contrast, the decreasing electronegativity of the chalcogen atoms as size increases would tend to stabilize the cationic charge inductively, predicting the opposite trend in stability. The thiopyrylium dye **5d** appears to be most stable to hydrolysis due to a combination of these effects, while the pyrlium dye **5a** appears to be less stable than one might predict from orbital overlap arguments alone.

Experimental Section

General Methods. Dyes **5** were prepared according to ref 5a. Aldehyde **12** was prepared according to ref 13. UV−visible−near-IR spectra were recorded on a Perkin-Elmer Lambda 12 spectrophotometer or on a Sequential DX17 MV stopped-flow spectrometer (Applied Photophysics, Leatherhead, UK). Both were equipped with a circulating constant-temperature bath for the sample chambers.

Preparation of Solutions for Kinetics Studies. Stock solutions of mono- (solution A, 1.50 M), di- (solution B, 0.5 M), and tribasic salts (solution C, 0.25 M) of potassium phosphate were used to prepare the buffer solutions with nearly constant values of [K^+] (0.53 ± 0.07 M) and μ (0.75 ± 0.15). Buffer solutions of approximately pH 4.5 were prepared from 400 mL of solution C and 600 mL of water ([K^+] 0.60 M, μ 0.60). Buffer solutions of approximately pH 6.0 were prepared from 197 mL of solution B, 235 mL of solution C, and 568 mL of water ([K^+] 0.55 M, μ 0.65). Buffer solutions of approximately pH 7.0 were

prepared from 430 mL of solution B, 70 mL of solution C, and 500 mL of water ($[K^+]$ 0.53 M, μ 0.75). Buffer solutions of approximately pH 8.0 were prepared from 500 mL of solution B and 500 mL of water ($[K^+]$ 0.50 M, μ 0.75). Buffer solutions of approximately pH 9.0 were prepared from 430 mL of solution B, 70 mL of solution C, and 500 mL of water ($[K^+]$ 0.50 M, μ 0.75). Buffer solutions of approximately pH 10.0 were prepared from 20 mL of solution A, 480 mL of solution B, and 500 mL of water ($[K^+]$ 0.49 M, μ 0.75). Buffer solutions of approximately pH 11.0 were prepared from 200 mL of solution A, 300 mL of solution B, and 500 mL of water ($[K^+]$ 0.45 M, μ 0.75). Buffer solutions of approximately pH 12.0 were prepared from 600 mL of solution A and 400 mL of water ($[K^+]$ 0.45 M, μ 0.90). Buffer solutions of approximately pH 3.5 were prepared from the pH 4.5 solution via the addition of 0.001 M HCl ($[K^+]$ 0.60 M, μ 0.60). An approximately pH 2.0 solution was prepared by adding 0.6 mol of KCl to 1 L of 0.01 M HCl ($[K^+]$ 0.60 M, μ 0.60). Slight adjustments to pH were made with dilute HCl to decrease pH and with dilute KOH to increase pH. Final pH measurements were determined on an Accumet Basic pH Meter (Fisher Scientific).

A 10-μL aliquot of a 0.03 M stock solution of dye in methanol was added to 3.0 mL of buffer (preheated to 310 K) in a 1-cm^2 quartz cuvette and the rate of loss of dye was recorded spectrophotometrically in a thermostated cell at 310.0 ± 0.1 K at λ_{max} for the dye. Values were measured in triplicate for rate constants agreeing within 5% and five or more times for rate constants where agreement was not within 5%. Conventional absorption spectroscopy was utilized with hydrolysis half-lives of ≥60 s and stopped-flow spectroscopy was used for faster reactions.

Phosphate concentrations were varied in the pH 8 buffer over a 4-fold range via dilution (0.06−0.25 M in dibasic phosphate), using KCl to maintain $[K^+]$ and μ. Over this range of buffer concentrations, values of k_{obs} for **5e** [$(1.2 \pm 0.3) \times 10^{-4}$ s^{-1}] and **5f** [$(3.7 \pm 0.6) \times 10^{-3}$ s^{-1}] were identical within experimental error. Contributions from k_{buffer} to k_{obs} were ignored.

Stopped-Flow Experiments. All stopped-flow experiments were performed on a Sequential DX17 MV stopped-flow spectrometer (Applied Photophysics, Leatherhead, UK). All experiments incorporated the instrument in stopped-flow mode only. The sample handling unit was fitted with two drive syringes that are mounted inside a thermostated-bath compartment, which allowed for constant temperature experimentation at 310.0 ± 0.1 K. The optical-detection cell was set up in the 10-mm path length. Curves were fitted using a Curfit subroutine that employed Marquardt algorithms. Absorption spectra at indicated time points were calculated through software provided by Applied Photophysics. This consisted of slicing at the appropriate time points across a series of kinetic traces (at different wavelengths) and then splining the points of a specific time group.

The solution of the dye for injection was prepared by diluting an aliquot of a stock solution in either MeOH or MeCN with either a dilute aqueous buffer (pH 5.4) or a solution of 0.005 M HCl in 44 wt % MeCN in water. The aliquot was adjusted to give a final concentration of the dye in the stopped-flow cell of $(5-7) \times 10^{-6}$ M. The other solution to be injected was either a concentrated aqueous buffer known to give a desired pH value upon mixing with the dye solution in dilute buffer or a solution of known concentration of KOH in 44 wt % MeCN in water.

Regeneration of Dyes 5a and 5b from Enediones 10a and 10b. A pH 8 buffer prepared as described above was diluted 100-fold (0.0025 M buffer). A 0.30 mL aliquot of a 1.0×10^{-3} M stock solution of either **5a** or **5b** was added to 2.7 mL of pH 8 buffer in a 1-cm quartz cuvette. The higher methanol content was to prevent any precipitation of the hydrolysis products from an all aqueous solvent. After two half-lives of hydrolysis, the cuvette was acidified with HPF_6 (transferred from the tip of a glass rod dipped in 60% HPF_6) and the reappearance either of **5a** (monitored at 595 nm) or of **5b** (monitored at 645 nm) was monitored over 2 h. The pH of the acidified solution was measured and was typically in the 3−4 range.

Acknowledgment. This research was supported by the National Institutes of Health (Grant No. NCI 1R01CA69155-01A1). The authors also thank Dr. Leo Fedor (SUNY Buffalo) for many helpful and insightful discussions.

JO980742Z